

Mechanical Properties of Trip Aided Bainitic Ferrite (TBF) Steels in Production and Service Conditions

Eren Billur^{1,2}, Semih Karabulut³, İmren Öztürk Yılmaz⁴, Samet Erzincanoğlu³, Hafize Çelik³, Evren Altınok³, Tanya Başer³

¹Atılım University, Metal Forming Center of Excellence, 06830, Ankara, TURKEY

²Billur Metal Form Ltd., 16120, Bursa, TURKEY

³TOFAŞ Türk Otomobil Fabrikası A.Ş., 16110, Bursa, TURKEY

⁴Beyçelik Gestamp A.Ş., 16110, Bursa, TURKEY

ABSTRACT

In the automotive industry, one of the most common methods to reduce the weight of the body components is to downgrade the sheets using higher strength steels. In the design phase, engineers typically use the material properties of the incoming material, such as the yield strength and the elongation. For forming analyses, however, more detailed characterization is required (flow curves, anisotropy, forming limit curves, etc.). Once the components are formed in the press shop, the yield strength increases due to work (strain) hardening. The parts are then welded in the body shop, and the body-in-white goes to the paint shop where it is baked to cure the paint. Most steels' yield strength changes during this paint bake cycle, which determines its final properties in service. Bake hardening (and in some cases, bake softening) is measured by Bake Hardening Index (BHI) as defined by EN 10325-2006. The standard dictates relatively low pre-strain (2%) and baking temperature (170°C). In real production conditions however, higher strains are achieved and baking temperatures may exceed 170°C to shorten the baking time. In this study, a new generation Advanced High Strength Steel (AHSS) grade TBF 1050 was characterized for metal forming purposes and its bake hardening response was studied both as the standard suggests and as the real production cycle dictates.

Keywords:

Advanced High Strength Steels; Material Characterization; Metal Forming; Elastic/Plastic Properties; Bake Hardening

INTRODUCTION

Automotive industry is under the pressure of complying government regulations of improved crash safety and low exhaust emissions [1]. To improve crash performance, additional reinforcements may be required, adding more weight to the car body [2]. Additional weight, in return, would increase the fuel consumption and thus increase exhaust emissions. To build safe and lightweight vehicles, materials with high strength to weight ratio are required [3].

High strength steels have been long used in the automotive industry and have replaced mild steels in most of the crash relevant components in the last decades. With "conventional" high strength steels (HSS), as the strength was increased the formability was reduced drastically, as seen in Fig. 1. The conventional HSS class involves various steel families including: (1) Bake Harde-

nable (BH), (2) Carbon-Manganese alloyed steels (CMn), and (3) High Strength Low Alloy (HSLA) grades [4]. These steels are single phase (ferritic) and have been dominating the crash components of cars until 1990's [5].

"Advanced" high strength steels (AHSS) consist of more than one phase and have been developed as early as 1970's [6]. It was mid 1990's, when cold rolled dual-phase (DP) steels were commercially available for the automotive industry [7]. These steels have ductile ferritic matrix with islands of hard martensite. The strength is increased by adjusting the alloying elements (mostly carbon) and/or the percentage of martensite [8].

Transformation Induced Plasticity (TRIP) steels were first defined in 1967 [9]. These steels have up to 15% retained austenite, which would transform to

Article History:

Received: 2017/11/14

Accepted: 2018/03/13

Online: 2018/09/30

Correspondence to: Eren Billur,
Atılım University, Metal Forming Center of
Excellence, 06830, Ankara, TURKEY
E-Mail: eren@billur.com.tr
Phone: +90 224 442 85 00

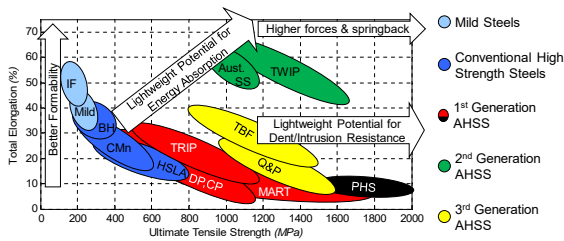


Figure 1. Steel banana curve, showing several different grades and classes.

martensite when plastically deformed. This so-called TRIP effect increases elongation [10]. Martensitic steels for cold (MART) and hot forming (Press hardened steel, PHS) are also classified as 1st generation AHSS. Currently PHS is the strongest steel family used in the automotive industry (up to 1300 MPa yield and 1800 MPa tensile strength), but requires a special hot forming line [4].

In 1998, Grässel and Frommeyer have developed Twinning Induced Plasticity (TWIP) steels [11]. These grades are classified as 2nd generation AHSS [5] and have very high elongation and strength. Over 60% total elongation was reported on a commercially available TWIP Steel with 500 MPa Yield and 980 MPa tensile strength [12]. Although seemed very promising, 2nd generation AHSS did not find many industrial applications, due to high material costs and poor weldability [13].

Since the beginning of the decade, automotive industry has been demanding high strength steels that have higher formability compared to 1st generation AHSS and less alloying elements compared to the 2nd generation [14]. Currently, Quenching & Partitioning (Q&P) steels and TRIP aided Bainitic Ferrite steels are commercially available and can be considered as 3rd generation AHSS [13].

This paper studies a TBF steel's mechanical properties in detail and also discusses the 'in-service' properties after work and bake hardening effects.

BACKGROUND

When a steel sheet is formed in the press shop, the strain-

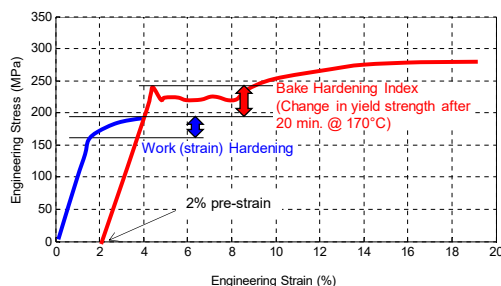


Figure 2. Work and bake hardening as explained in the standard (re-created after [20]).

ning would increase the yield strength and hardness; and reduces the ductility. This is called strain hardening (also known as work hardening) [15]. Work hardening of a material can be easily measured by a simple tensile test. In TRIP steels and TRIP-aided steels, very high strain hardening is observed until the uniform elongation [16]. This can be explained by the localized high strain hardening rate, caused by formation of mobile dislocations and the transformation of retained austenite to martensite [17, 18].

In press shops, when a steel is deformed its thickness is reduced, but its yield strength is increased by work hardening. Typically, in computer-aided-engineering (CAE) calculations, both of these effects are included. For example, NVH and crash simulations include both thinning and hardening effects. However, bake hardening effect was mostly discarded [19].

Bake hardening is the increase of yield stress after deformation, followed by a baking cycle. Bake hardenability of a steel is typically measured by tensile test [3], according to EN 10325-2006 standard [20]. Fig. 2 summarizes how the "Bake Hardening Index" is measured. According to the standard, the deformation is limited to 2% pre-strain (engineering) and baking cycle is at 170°C for 20 minutes.

Since there is a class of "Bake Hardenable" steels, one may think that other high strength steels do not harden during bake cycle. In reality, most AHSS grades also harden after baking. In most steel datasheets, bake hardening index is given as a material property. For a given dual phase steel (cold rolled DP590, CR330Y590T-DP) for example, most steel makers claim a minimum 30 MPa bake hardening index (BHI as shown in Fig. 2, sometimes abbreviated as BH₁) [21, 22, 23].

However, former studies have shown that even at 2% pre-strain, much higher BHI was achieved. A study by Volvo for example, showed that the yield strength of DP1000 was increased from 760 to 1020 MPa after work and bake hardening. Similarly, the yield strength of DP1200 was increased from 950 to 1220 MPa [24].

In another study by Salzgitter, tensile specimens cut from real automotive components were tested. Results are tabulated in Table 1. Since the pre-strain was not kept constant, but changed with the part complexity, work hardening numbers were not constant [25].

Since the new generation AHSS have higher formability compared to steels with similar yield strength; the part complexity and thus the pre-strain could be even higher. Effect of pre-strain was known and studied as early as 1990's

Table 1. Summary of work and bake hardening, samples were cut from press formed automotive components, made of DP590 (CR330Y590T-DP) [25].

Part and thickness	Work hardening (MPa)	Bake hardening (MPa)
Seat cross member, 1.0 mm	179-189	52-59
A-pillar lower, 2.0 mm	66-67	131-137
D-pillar reinforcement, 1.0 mm	206-210	52-79

[26]. However, most of the early works had limited pre-strain. A summary of several studies on pre-strain is given in Fig. 3 [26, 27, 28, 29].

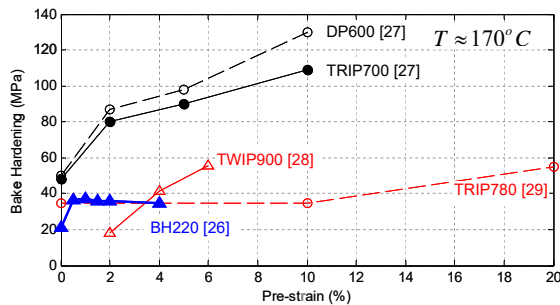


Figure 3. Bake hardening responses of several HSS and AHSS with varying pre-strain [26-29].

Lastly, the standard dictates that the bake hardening studies should be done at 170°C. However, in manufacturing conditions, temperature in the paint bake tunnel may increase over 200°C. Typically if the furnace temperature exceeds 170°C, the baking time could be reduced, as long as the time-temperature profile is within the acceptable region, as shown in Fig. 4 [30]. This is of extreme importance, as the paint shops are typically the bottleneck of a car maker. The capacity of the total production is generally limited by the paint shop. If the cycle time here could be reduced, the overall productivity could be boosted [31].

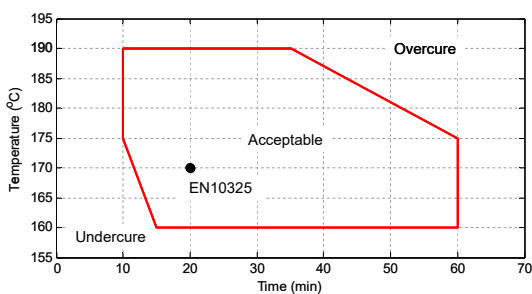


Figure 4. An example e-coat curing bake chart [30].

A special condition in bake hardening of TBF steels is the fact that, they contain ferrite, bainite, martensite and retained austenite. It is reported that from these phases bainite contributes most to BH response. It is also possible that some fraction retained austenite may transform due to holding at high temperature for several minutes, or the martensite may be tempered [16, 27]. According to [32], the amo-

unt of retained austenite does not change with temperatures up to 170°C for a TRIP 700 steel. Only after 700 minutes holding at 220°C, the retained austenite fraction started to decrease in the aforementioned steel.

Several studies in the literature has also shown that with increased baking temperature, higher bake hardening response could be determined [26, 28]. In this study, (1) TBF steels are studied, and (2) the baking time was reduced with increased baking temperature.

EXPERIMENTAL STUDIES

In this study, commercially available, cold rolled TBF 1050 steels are studied at two different thickness levels: 1.0 and 1.6 mm. These steels were characterized using:

- 1) Tensile tests with extensometers to determine, yield strength and Lankford parameters in three directions (r_0 , r_{45} , r_{90});
- 2) Elemental analysis to determine chemical composition;
- 3) Elastic modulus determination by Resonance Frequency and Damping Analysis (RFDA);
- 4) Disk compression test to determine biaxial yield stress (σ_p) and anisotropy coefficient (r_p);
- 5) Bake hardening experiments at 0%, 2%, 5% and 10% pre-strain; at various “industry emulating” temperatures and durations.

Tensile Tests

Tensile specimens were manufactured using wire EDM method to minimize the damage at the edges. Tests were conducted at two crosshead speeds: 30 mm/min and 150 mm/min. Although there was no strain rate control, these crosshead speeds gave relative constant true strain rate levels of: $(3.75 \pm 0.10) \times 10^{-3}$ and $(18.3 \pm 0.2) \times 10^{-3} \text{ s}^{-1}$. As illustrated in Fig. 5, the yield strength was found to be sensitive to the strain rate; whereas the ultimate tensile strength was predominantly affected by the thickness.

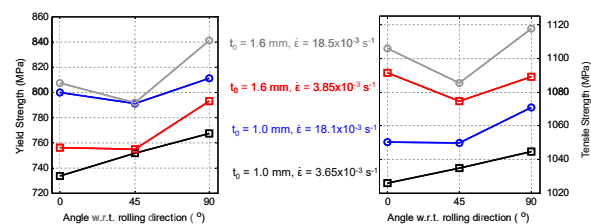


Figure 5. Yield and ultimate tensile strength of TBF 1050 steels.

Table 2. Summary of tensile tests, compared with the literature [33, 34].

	Experiments		Literature	
	$t_o = 1.0 \text{ mm}$	$t_o = 1.6 \text{ mm}$	Datasheet [29]	$t_o = 1.2 \text{ mm}$ [30]
Yield Strength (MPa) ^a	751 ⁺¹⁷ ₋₁₇	800 ⁺¹⁰ ₋₁₀	700-820	775
UTS (MPa) ^a	1035 ⁺¹⁰ ₋₁₀	1057 ⁺¹⁴ ₋₇	1050-1180	1235
Elongation (%) ^a	17 ^{+0.7} _{-0.7}	13.5 ^{+1.2} _{-0.9}	≥14	10
r_o	0.778	0.786	-	0.795
r_{45}	0.905	0.958	-	0.930
r_{90}	0.995	0.911	-	0.983

^aValues determined from slow strain rate experiments.

Material properties found in this study are tabulated and compared with the literature in Table 2.

Elemental analysis

Elemental analysis was performed on 1.0 mm thick steels, using Bruker Q4 optical emission spectrometer. Samples were measured 10 times, at different locations. The results were compared with the literature in Table 3.

Table 3. Chemical composition (wt.%) of TBF 1050, compared with literature [33, 34].

wt. %	C	Mn	Si	P	Al
This study	0.203 ^{+0.034} _{-0.021}	2.253 ^{+0.194} _{-0.197}	1.027 ^{+0.194} _{-0.096}	0.015 ^{+0.004} _{-0.004}	0.045 ^{+0.009} _{-0.007}
Datasheet [34]	<0.23	<2.3	<2	-	-
Literature [35]	0.207	2.178	1.452	0.021	0.037

Elastic modulus measurement using RFDA

Elastic modulus measurement was done using impulse excitation and resonant frequency and damping analyser (RFDA) system. In this method, a rectangular specimen is placed on two supporting wires. An impulse excitation is given by the system, and a microphone records the vibrations. Through signal processing, elastic properties of a specimen could be determined. Details of the methodology and the system used in this study can be studied in detail from reference [35]. In this study, 55x10 mm specimens were prepared using wire EDM. 4 test specimens were produced for each thickness. Results are tabulated in Table 4.

Table 4. Elastic modulus measurements.

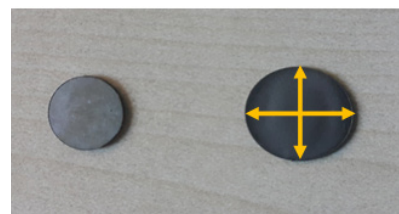
Elastic Modulus (GPa)	Thickness	
	1.0 mm	1.6 mm
Test 1	192.77	189.08
Test 2	192.68	189.14
Test 3	192.50	188.21
Test 4	192.43	189.17
Average	192.60 ^{+0.17} _{-0.17}	188.90 ^{+0.27} _{-0.69}

Disk compression tests

For metal forming simulations, yield locus is one of the most important input data. To build some of the modern yield loci (such as Yld2000 or Banabic 2005), biaxial anisotropy coefficient (r_b) and biaxial yield strength (σ_b) are required [36, 37]. A method to determine these coefficients is disk compression test [38].

10 mm diameter disks were cut using wire EDM tech-

nique. These are then compressed in a universal tensile machine. The final disks became elliptical, and the ratio



$$r_b = \frac{\epsilon_{22}}{\epsilon_{11}},$$

$$\epsilon = \ln\left(\frac{D_f}{D_i}\right)$$

Figure 6. Calculation of biaxial anisotropy coefficient (after [37]).

between the strains gives the biaxial anisotropy coefficient, as summarized in Fig. 6. Calculated values are given in Tab-

Table 5. Biaxial anisotropy coefficients.

Applied Force	Thickness	
	1.0 mm	1.6 mm
150 kN	$D_{f1} = 10.99 \text{ mm}$	$D_{f1} = 10.71 \text{ mm}$
	$D_{f2} = 10.91 \text{ mm}$	$D_{f2} = 10.61 \text{ mm}$
	$r_b = 0.922$	$r_b = 0.863$
200 kN	$D_{f1} = 11.70 \text{ mm}$	$D_{f1} = 11.25 \text{ mm}$
	$D_{f2} = 11.50 \text{ mm}$	$D_{f2} = 11.18 \text{ mm}$
	$r_b = 0.890$	$r_b = 0.947$
Average r_b	0.906	0.905

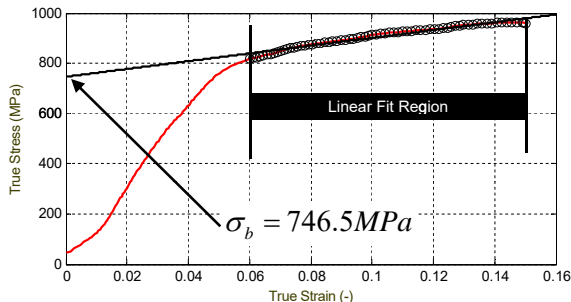


Figure 7. Calculation of biaxial yield strength (after [37]).

le 5. The biaxial yield strength is calculated using a linear fit [37], as shown in Fig. 7.

Bake hardening studies

As discussed in earlier sections, in this study: (1) higher pre-strains and (2) realistic furnace conditions were studied. Since the tensile tests have shown that the parts can be deformed 12.6-17.7% total elongation (see Table 2), the maximum pre-strain was selected to be 10%. The tensile specimens were pre-strained to 2, 5 and 10% using a universal tensile test machine. Specimens were then placed in the furnace which is already pre-heated to the temperatures listed in Table 6. Furnace temperature and

Table 6. Details of the bake hardening conditions.

Conditions	Furnace Temp. (°C)	Dwell time (min.)	Reference
1	170	20	EN10325 [20]
2	195	15	Tofaş
3	205	15	Tofaş

dwell time data are received from Tofaş. To compare the results, conditions of EN10325 were also studied. Once the specimens stay in the furnace for the given time, they were taken out. The specimens were air cooled to room temperature and tensile tests were performed until fracture. Results of one test conditions can be seen in Fig. 8.

As seen in Fig. 8, when the tensile curves are shifted with pre-strain, the difference between the “as-received”

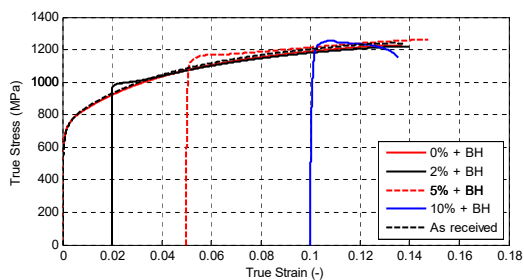


Figure 8. Tensile test results after pre-strain and bake hardening (1.0 mm thick blanks, 170°C furnace temperature, 20 minutes dwell time).

curve and the tested material’s curve gives the bake hardening. To calculate the work hardening, it is possible to use the stress level on the “as-received” curve and subtract the yield strength of the corresponding material (i.e., 1.0 mm or 1.6 mm thick). Work hardening values were quite repeatable. This can be seen in Fig. 9a-b.

With only two exceptions, as pre-strain and as temperature is increased, the bake hardening was found to be increasing. In addition, the bake hardening response of TBF steels was found to exceed 200 MPa, when 10% pre-strain is applied. Even at 5% pre-strain, 1200 MPa yield strength could be achieved after bake hardening.

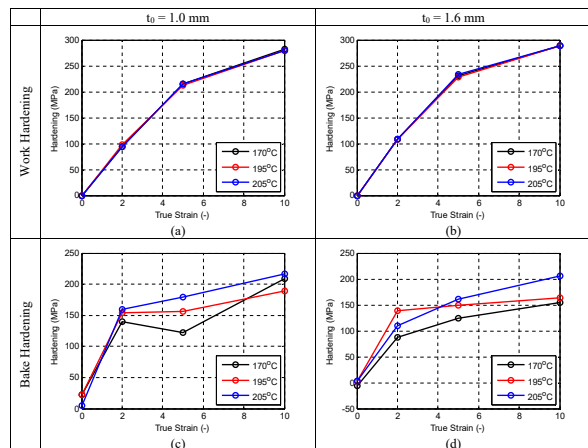


Figure 9. Summary of work and bake hardening at different conditions.

CONCLUSION

In this study, a commercially available 3rd generation AHSS grade had been selected and its elastic/plastic properties were characterized, including its bake hardening response. It has to be noted that these values are only from one batch of one producer.

Elemental analyses have proved that 3rd generation AHSS had relatively low alloying elements, especially compared to 2nd generation AHSS. As the blank has low carbon equivalency, its welding parameters are expected to be compatible with current body shops. A further study on weldability is currently ongoing.

Further analysis on the phase fractions (especially retained austenite) is required to understand how the changes in phase fractions may have effect on the hardening, anisotropy and bake hardening responses.

Elastic modulus of these steels was found to be on the lower side of steels. This information may be useful for further studies about springback of these grades.

Biaxial material properties as required by some yield criterion were measured by disk compression test. Currently there is no literature data to compare these results. In future, these values could be used to build YLD2000-2D or BBC2005 yield criteria; and by using finite element simulations, the material model could be validated.

One of the main purposes of using cold formable advanced high strength steels is to reduce press hardened steels (PHS). It was clearly found that after press forming and bake hardening, this grade may have a yield strength over 1200 MPa. This is comparable to PHS, which would require a special hot forming line and expensive process.

ACKNOWLEDGEMENT

This study has been supported by Turkish Science Foundation (TÜBİTAK), Project number: 3150934. Authors would like to thank Mr. Emin Tamer and Asst. Prof. Dr.-Ing. Kemal Davut of Atılım University Metal Forming Center of Excellence for their help in experimental work.

References

1. Taub AI, Luo AA, Advanced lightweight materials and manufacturing processes for automotive applications. *MRS Bulletin* 40/12 (2015) 1045-1054.
2. Robert H and Scherre JM, New Peugeot 3008. Proceedings of EuroCarBody 2016, (2016), Bad Nauheim, Germany.
3. Senuma T, Physical Metallurgy of Modern High Strength Steel Sheets, *ISIJ International* 41/6 (2001) 520-532.
4. Billur E, Altan T, Three generations of advanced high-strength steels for automotive applications, Part I. *Stamping Journal*, Nov-Dec., (2013) 16-17.
5. Pichler A, Hebesberger T, Krizan D, Winkelhofer F, Fruber M, Walch C, 3rd Generation of AHSS Grades: A New Family of Steel Grades with a Significantly Improved Balance between Strength and Formability. Proceedings of Materials in Car Body Engineering 2014, (2014), Bad Nauheim, Germany.
6. Araki K, Takada Y, Nakaoka K, Work hardening of continuously annealed dual phase steels. *Trans. Iron Steel Inst. Jpn.* 17/12 (1977) 710-717.
7. ThyssenKrupp Stahl AG, Höherfester Stahl für den Automobil-Leichtbau. ThyssenKrupp Stahl, No: 2045, (1999), Duisburg.
8. Ramazani A, Bruehl S, Gerber T, Bleck W, Prah U, Quantification of bake hardening effect in DP600 and TRIP700 steels. *Materials & Design* 57/C (2014) 479-486.
9. Zackay VF, Parker ER, Fahr D, Busch R, The enhancement of ductility in high-strength steels. *ASM Trans Quart* 60/2 (1967) 252-259.
10. Samek L, Krizan D, Steel-material of choice for automotive lightweight applications. *Metal Review* (2012) 1-6.
11. Grässel O, Frommeyer G, Effect of martensitic phase transformation and deformation twinning on mechanical properties of Fe-Mn-Si-Al steels. *Materials Science and Technology* 14/12 (1998) 1213-1217.
12. Billur E, Çetin B, Uğuz RO, Davut K, Arslan E, Advanced Material Characterization of TWIP Steels. Proceedings of New Developments in Sheet Metal Forming (2016) 303-318.
13. Davenport M, Third-generation advanced high strength steel emerges, *Stamping Journal*, Sept.-Oct., (2017) 22-28.
14. Branagan D, Overview of a New Category of 3rd Generation AHSS. Presented at Great Designs in Steel 2013, May 1, Livonia, MI, USA 2013.
15. Altan T, Tekkaya AE. Sheet metal forming: processes and applications, ASM International, 2012, ISBN:978-1615038442.
16. Fonstein N. Advanced High Strength Sheet Steels, Springer, 2015.
17. Sugimoto K, Mukherjee M, Chapter 8 - TRIP aided and complex phase steels, in: *Automotive Steels*, Rana R, Singh, SB (eds.) Woodhead Publishing, pp. 217-257, 2017.
18. Li SH, Dan WJ, Zhang WG, Lin ZQ, A model for strain-induced martensitic transformation of TRIP steel with pre-strain, *Computational Materials Science* 40/2 (2007) 292-299.
19. Stillger M, Brenne T, Feasibility-Simulation and Systematic Process Improvement of Hot Forming Parts as well as Mapping of Results to Vehicle Simulation, in: *Proceedings of New Developments in Sheet Metal Forming 2016 (NEBU 2016)*, pp. 213-230, 2016.
20. European Committee for Standardization, EN 10325:2006: Steel - Determination of yield strength increase by the effect of heat treatment [Bake-Hardening-Index], 2006.
21. ArcelorMittal, Dual Phase Steels,, Product Brochure, 2017.
22. SSAB, Docol 590DP,, Product Brochure, 2017.
23. Voestalpine Steel Division, Dual-Phase Steels,, Product Brochure, 2017.
24. Jonason, P, Aluminium intensive door - Mixmetal door structure, Presented at Doors and Closures in Car Body Engineering 2010, Bad Nauheim, Germany, 2010.
25. Flaxa V, Schulz T, Schulz S, Mohrbacher H, Entwicklung eines modularen Legierungskonzeptes für HDG DP-Stähle nach VDA239, 2013.
26. Pradhan, R, Dent-Resistant Brake-Hardening Steels for Automotive Outer-Body Applications, in SAE Technical Paper, SAE:910290, 1991.
27. Pereloma E, Timokhina I, Chapter 9 - Bake hardening of automotive steels, in *Automotive Steels*, Rana R, Singh, SB (eds.) Woodhead Publishing, pp. 259-288, 2017.
28. Kilic S, Ozturk F, Sigirtmac T, Tekin G, Effects of Pre-strain and Temperature on Bake Hardening of TWIP900CR Steel, *Journal of Iron and Steel Research* 22/4 (2015) 361-365.
29. Robertson LT, Hilditch TB, Hodgson PD, The effect of prestrain and bake hardening on the low-cycle fatigue properties of TRIP steel, *International Journal of Fatigue* 30/4 (2008) 587-594.
30. Dickie RA, Bauer DR, Ward SM, Wagner DA, Modeling paint and adhesive cure in automotive applications, *Progress in Organic Coatings* 31/3 (1997) 209-216.
31. Weenink W, Car Plants Order New Paint Shops, *Automotive News Europe*, 23 June 1997.
32. Bleck W, Bruhl S, Bake hardening effects in advanced high strength steels. In *New Development on Metallurgy and Applications of High Strength Steels*, 2008.
33. ArcelorMittal, Steels for cold stamping -Fortiform®, Product Brochure, 2014.
34. Galdos L, de Argandoña ES, Mendiguren J, Gil I, Ulibarri U, Mugarra, E, Numerical simulation of U-Drawing test of Fortiform 1050 steel using different material models, *Procedia Engineering* 207 (2017) 137-142.
35. Bollen B, The Impulse Excitation technique., in *AMAP Colloquium*, Aachen, Germany, 2017.
36. Banabic D, Sester M, The Influence of the Constitutive Equations on the Accuracy of Sheet Metal Forming Processes Simulation, in *Die and Mold*, Ankara, Turkey, 2011.

37. Xu L, Barlat F, Disk compression testing and constitutive modeling of TWIP sheet sample. In: Proceedings of ICTP (2008) 2312-2317.
38. Barlat F, Brem JC, Yoon JW, Chung K, Dick RE, Lege DJ, Pourboghrat F, Choi S-H, Chu E, Plane stress yield function for aluminum alloy sheets—Part 1: Theory, International Journal of Plasticity 19/9 (2003) 1297-1319.